Expression, Site-Directed Mutagenesis, and Steady State Kinetic Analysis of the Terminal Thioesterase Domain of the Methymycin/Picromycin Polyketide Synthase[†]

Hongxiang Lu,[‡] Shiou-Chuan Tsai,[§] Chaitan Khosla,[§,||,⊥] and David E. Cane*[,‡]

Department of Chemistry, Brown University, Box H, Providence, Rhode Island 02912-9108, and Departments of Chemical Engineering, Chemistry, and Biochemistry, Stanford University, Stanford, California 94305-5025

Received April 24, 2002; Revised Manuscript Received July 17, 2002

ABSTRACT: The thioesterase (TE) domain of the methymycin/picromycin synthase (PICS) was functionally expressed in *Escherichia coli*, and the optimal N-terminal boundary of the recombinant TE was determined. A series of diketide-*N*-acetylcysteamine (SNAC) thioesters were tested as substrates. PICS TE showed a strong preference for the 2-methyl-3-ketopentanoyl-SNAC substrate **5** over the stereoisomers of the reduced diketides **1**−**4**, with an ∼1.6:1 preference for the (2*R*,3*S*)-2-methyl-3-hydroxy diastereomer **2** over the (2*S*,3*R*)-diketide **1**. The closely related DEBS TE, the thioesterase from the 6-deoxyerythronolide B synthase, showed a more marked 4.4:1 preference for **2** over **1**, with only a slightly greater preference for the 3-ketoacyl-SNAC substrate **5**. The roles of several active site residues in PICS TE were examined by site-directed mutagenesis. Serine 148, which is part of the apparent catalytic triad consisting of S148, H268, and D176, was found to be essential for thioesterase activity, while replacement of D176 with asparagine (D176N) gave a mutant thioesterase that retained substantial, albeit reduced, hydrolytic activity toward diketide-SNAC substrates. Mutation of E187 and R191, each of which is thought to play a role in substrate binding, had only minor effects on the relative specificity for diketide substrates **1**, **2**, and **5**. Finally, when PICS TE was fused to the C-terminus of DEBS module 3, the resultant chimeric protein converted diketide **1** with methylmalonyl-CoA to triketide ketolactone **6** with improved catalytic efficiency compared to that of the previously developed DEBS module 3−(DEBS)TE construct.

Modular polyketide synthases (PKSs)[1] are a family of multifunctional megaproteins that catalyze the biosynthesis of the aglycone cores of numerous polyketide natural products, including the broad spectrum antibiotic erythromycin A and the immunosuppressant rapamycin (*1*, *2*). Typical of such enzymes is the methymycin/picromycin synthase (PICS) of *Streptomyces venezuelae* (Figure 1) which mediates the formation of 10-deoxymethynolide and narbonolide, the parent aglycones of the macrolide antibiotics methymycin and picromycin, respectively (*3*, *4*). PICS is organized into six groups of coordinated active sites known as modules, each of which is responsible for a single round of polyketide chain elongation and functional group modification. Each module is made up of a group of covalently linked, catalytically functional protein domains, among which the core domains are a ketosynthase (KS), an acyltransferase (AT), and an acyl carrier protein (ACP) domain. The AT domain is responsible for the transfer of a specific chain extender unit, such as methylmalonyl-CoA or malonyl-CoA, onto the terminal thiol residue of the pantetheinyl side chain of the ACP domain. The KS domain then catalyzes a decarboxylative condensation of the methylmalonyl- or malonyl-ACP thioester with the acyl group of the growing polyketide chain, by a mechanism similar to that of fatty acid biosynthesis. Variable combinations of additional catalytic domains within each module are responsible for modification of the initially generated polyketide chain by 3-keto acyl thioester reduction (KR domain), dehydration (DH domain), and enoyl acy thioester reduction (ER domain). The resultant elongated polyketide intermediate is then passed to a specific downstream module which then carries out another round of condensation and functional group modification. A dedicated loading domain, located at the N-terminus of PICS module 1, consists of an additional ACP domain, a specialized AT domain, and a modified KS^Q domain that together decarboxylate methylmalonyl-CoA and load the resultant propionyl residue onto the active site cysteine of the KS domain of module 1 (KS1). The successive rounds of chain elongation continue until the final module has carried out its specific set of reactions to generate the mature polyketide, attached to the corresponding ACP domain. The polyketide is then released from the ACP with concomitant macrolactonization, in a reaction catalyzed by a unique thioesterase (TE) domain located at the C-terminus

[†] This research was supported by grants from the National Institutes of Health to D.E.C. (GM22172) and C.K. (CA66736).

* To whom correspondence should be addressed. E-mail: David_Cane@Brown.edu. Telephone: (401) 863-3588. Fax: (401) 863-3556.

[‡] Brown University.

[§] Department of Chemical Engineering, Stanford University.

[||] Department of Chemistry, Stanford University.

[⊥] Department of Biochemistry, Stanford University.

[1] Abbreviations: ACP, acyl carrier protein; AT, acyltransferase; DEBS, 6-deoxyerythronolide B synthase; DH, β-hydroxyacyl-ACP dehydratase; ER, enoyl-ACP reductase; KR, β-ketoacyl-ACP reductase; KR°, inactive KR; KS, β-ketoacyl-ACP synthase; KS^Q, KS-like domain in which the active site Cys has been replaced with Gln; PICS, picromycin synthase; PKS, polyketide synthase; TE, thioesterase; SNAC, *N*-acetylcysteamine; 6-dEB, 6-deoxyerythronolide B.

10.1021/bi026006d CCC: $22.00
Published on Web 09/27/2002

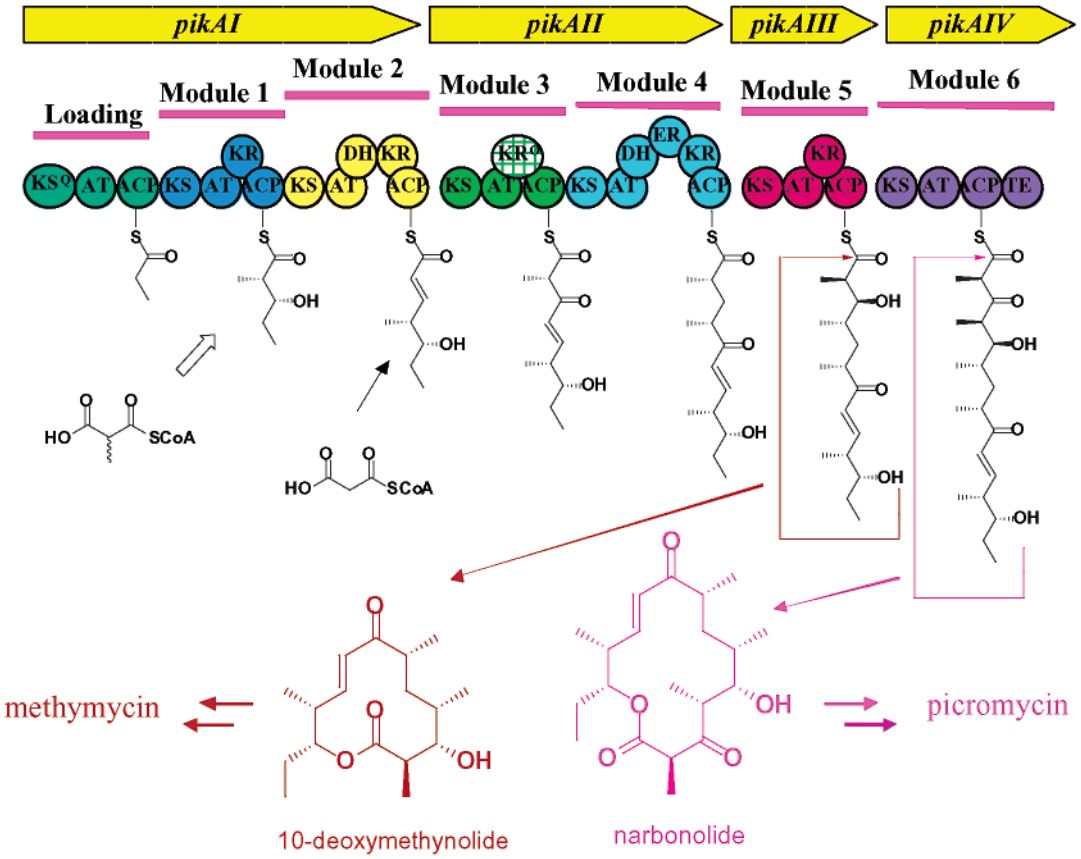

FIGURE 1: Biosynthesis of 10-deoxymethynolide and narbonolide by the methymycin/picromycin synthase (PICS). The loading domain is primed with the starter propionyl unit, by acylation of the ACP domain with methylmalonyl-CoA followed by a decarboxylation catalyzed by the KS^Q. All other modules except module 2 use methylmalonyl-CoA as the extender unit, while module 2 is specific for malonyl-CoA. The TE domain at the C-terminus of module 6 catalyzes the macrolactonization of hexaketide and heptaketide substrates generated by modules 5 and 6, respectively, to give 10-deoxymethynolide and narbonolide. Each of these aglycones is further modified by other enzymes to give methymycin and picromycin, respectively.

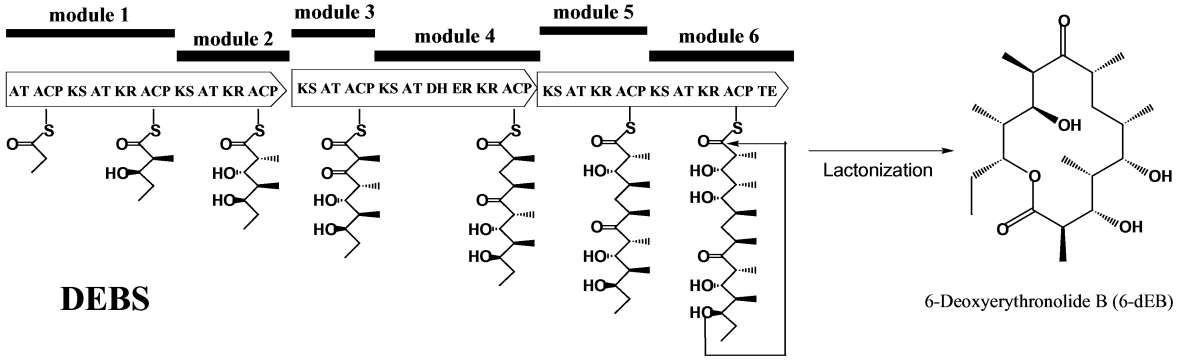

FIGURE 2: Formation of 6-deoxyerythronolide B (6-dEB) by 6-deoxyerythronolide B synthase (DEBS). The DEBS TE domain releases the mature heptaketide from the ACP domain of DEBS module 6 by lactonization to give 6-dEB.

of the sixth module, just downstream of the ACP domain. The entire cycle of polyketide chain elongation reactions is very similar to that mediated by 6-deoxyerythronolide B synthase (DEBS, Figure 2), a closely related modular PKS the mechanism of action, substrate specificity, and module organization of which have been studied in great detail (*2*, *5*).

PICS differs from other known polyketide synthases in generating polyketides of two different chain lengths, the hexaketide 12-membered ring 10-deoxymethynolide (*6*) and the heptaketide 14-membered ring narbonolide. In cultures of *S. venezuelae*, the proportions of the two macrolactone products can be varied according to the culture conditions (*6*, *7*). It has been shown by Sherman that the formation of the immature 10-deoxymethynolide is due to the expression of an N-terminally truncated form of module 6 in which a portion of the PICS KS6 domain has been deleted (*7*). In the latter case, the TE domain acts on the hexaketide product generated by PICS module 5. Interestingly, heterologous expression of PICS in *Streptomyces lividans* also gives rise to macrolides of both ring sizes, indicating that differential translation of PICS module 6 (*picAIV*) open reading frame is independent of any host specific factors in *S. venezuelae* (*4*). Both of the two macrolide aglycones are normally further glycosylated and oxidized by the same set of enzymes to yield methymycin and picromycin, respectively (*8*−*11*).

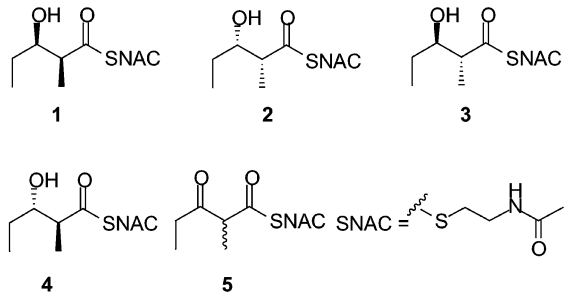

FIGURE 3: Diketide substrates of PICS TE and DEBS TE.

The thioesterase domain of the DEBS polyketide synthase is closely related in amino acid sequence and in function to PICS TE. Although DEBS TE normally catalyzes the formation of the 14-membered macrolactone, 6-deoxyerythronolide B, this same domain has considerable substrate flexibility, as shown by its ability to catalyze the formation of 6-, 8-, 12-, and 16-membered lactones when fused to the C-terminus of various DEBS modules (*2*, *12*, *13)*. DEBS TE has been expressed in *Escherichia coli*, either as a single domain (*14*) or fused to the DEBS ACP6 domain (*15*, *16*). The substrate specificity of recombinant DEBS TE has been investigated using *N*-acetylcysteamine (SNAC) thioesters as model substrates, revealing a kinetic preference for hydrolysis of (2*R*,3*S*)-2-methyl-3-hydroxyacyl thioesters such as the diketide **2** over the (2*S*,3*R*)-enantiomer **1**, as well as long-chain acyl thioesters over shorter chain substrates (*14*) (Figure 3). None of the substrate analogues examined to date have been converted to lactone products. The thioesterase-catalyzed reaction is thought to involve nucleophilic catalysis by an active site serine, a conclusion supported by the detection of covalent acyl−enzyme adducts by electrospray mass spectrometry when diketide *p*-nitrophenyl oxoesters were used as substrates (*16*). The three-dimensional structure of DEBS TE has recently been determined, revealing the thioesterase protein to be a dimer with an unusual open substrate channel that traverses each subunit (*17*).

We now report the heterologous expression of PICS TE, the comparison of its intrinsic substrate specificity with that of DEBS TE, and the investigation by site-directed mutagenesis of the role of selected active site residues. The following paper (*18*) reports the determination of the structure of the PICS TE and the discovery of pH-dependent changes in the size of the substrate channels of both PICS TE and DEBS TE.

EXPERIMENTAL PROCEDURES

Materials and General Methods. Restriction enzymes and T4 DNA ligase were purchased from New England Biolabs. The synthesis of the four diastereomers of diketide-SNAC **1**−**4** and 3-keto-diketide-SNAC **5** has been reported previously (*19*−*21*). Oligonucleotide primers were purchased from Integrated DNA Technologies. DNA sequencing of PCR products was performed on double-stranded plasmids by the HHMI Biopolymer/Keck Foundation Biotechnology Resource Laboratory at the Yale University School of Medicine (New Haven, CT). Reagents for kinetic assays and chemical synthesis were purchased from Sigma-Aldrich Chemical Co. and were of the highest available grade. Culture medium components were obtained from Difco.

Construction of Expression Plasmids for PICS TE and Mutants. Since the exact N-terminal start of the PICS TE domain is unknown, the open reading frame was amplified by PCR using three different forward primers to introduce N-terminal codons at various positions in the linker region between ACP6 and the actual TE domain. The template for PCR was plasmid pKOS039-86 (*4*) harboring the complete cluster of PICS genes, *pikAI*−*pikAIV* (GenBank accession no. AF079138), which was provided by R. McDaniel of Kosan Biosciences, Inc. The forward primers for the three PCR constructs *te1*−*te3* were 5′-AGT GAG T**CA TAT G**TG GGC CGT CGC CGA GCC GTC-3′, 5′-AGT GAG T**CA TAT G**TC CGG GGC CGA CAC CGG CG-3′, and 5′-AGT GAG T**CA TAT G**CT CGA CCC GGT GCT GCT CGC CG-3′, respectively, with the engineered *Nde*I site shown in bold. The reverse primer for all three amplifications was 5′-AGT GAG T**GG ATC C**TC ACT TGC CCG CCC CCT CGA T-3′ which introduced a *Bam*HI site (bold) adjacent to the TCA complement (underlined) of the natural stop codon TGA. The resultant PCR products (*te1*−*te3*) corresponded to bp 3073−4041, 3145−4041, and 3298−4041 of *pikAIV*, respectively. The PCR was carried out using *pfu* turbo polymerase (Stratagene) with 9% DMSO in the reaction mixture with cycling conditions recommended by the manufacturer. The resulting PCR products were purified and digested with *Nde*I and *Bam*HI and then ligated into the expression vector pET-28a (Novagen) to produce plasmids pHL4-65a, pHL4-65b, and pHL4-65c, respectively.

Plasmid pHL5-81, in which the *te2* gene in pHL4-65b had been subcloned into *Nde*I- and *Bam*HI-digested pBluescript KSII (Novagen), was used as the template for site-directed mutagenesis. Mutants were prepared using the QuickChange Site-Directed Mutagenesis Kit (Stratagene). The double mutant E187N/R191E was prepared by first introducing the R191E mutation into the PICS TE gene and then carrying out a second round of PCR mutagenesis. As an example, the primers used to generate the PICS TE D176N mutant were 5′-GCC GGG ATC GTC CTG GTC AAC CCC TAT CCG CCG GGC CAT C-3′ and 5′-GAT GGC CCG GCG GAT AGG GGT TGA CCA GGA CGA TCC CGG C-3′ (complementary mutation sequences are underlined). The PCR reaction mixture contained 9% DMSO and used 17 cycles of amplification: denaturation at 96 °C for 30s, annealing at 52 °C for 1 min, and extension at 68 °C for 10 min. The resultant product mixture was then supplemented with 0.02 unit/μL *Dpn*I and incubated at 37 °C for 1 h prior to transformation of *E. coli* XL10-Gold ultracompetent cells (Stratagene). Individual colonies that grew on LB−agar plates supplemented with 100 μg/mL ampicillin were used to inoculate a 1 mL overnight culture of LB containing 100 μg/mL ampicillin. The plasmid encoding the desired mutation was isolated, digested with *Nde*I and *Bam*HI, and cloned back into the pET-28a vector for expression. All the other mutants were prepared with the same method. Primers and PCR cycle conditions are listed in the Supporting Information.

Expression and Purification of Wild-Type and Mutant PICS TE. pHL4-65a, pHL4-65b, and pHL4-65c, as well as each of the plasmids harboring mutations in PICS TE, were transformed into *E. coli* BL21(DE3)/pLysS (Stratagene) for protein expression. The pET28a introduces an N-terminal His_6 tag into the resultant protein. Expression and purification procedures were the same for both wild-type PICS TE and

each mutant. A 200 mL culture of *E. coli* BL21(DE3)/pLysS harboring the appropriate plasmid was grown at 37 °C in a 1 L flask using LB medium supplemented with 50 μg/mL kanamycin to an OD_{600} of 0.8. After induction of protein expression by addition of 1 mM IPTG, incubation was continued for 12 h at 20 °C.

All protein purification procedures were performed at 4 °C. The cells were harvested by centrifugation at 4000*g*, washed once with 20 mL of 50 mM phosphate buffer (pH 8.0), and collected again by centrifugation at 9000*g*. After suspension in 15 mL of 200 mM sodium phosphate buffer (pH 7.2) containing 200 mM sodium chloride, 2.5 mM dithiothreitol, 2.5 mM EDTA, 1.5 mM benzamidine, 30% glycerol (v/v), and 2 mg/L pepstatin and leupeptin, the cells were disrupted by being passed through a French press at 16 000 psi. The resulting cell lysate was treated with 1 mg/mL DNaseI (25 mM $MgCl_2$) for 20 min, followed by DNA precipitation with 0.15% polyethylenimine for 20 min. The cell debris and precipitated DNA were removed by centrifugation at 53000*g*. The supernatant was diluted 2-fold with buffer A [100 mM sodium phosphate (pH 7.2), 0.5 M NaCl, 20% glycerol, and 20 mM imidazole] and mixed with the appropriate amount of His-Bind resin (Novagen, resin binding capacity, 8 mg of His-tagged protein/mL of resin) for 40 min. The protein was eluted from the resin with buffer B [100 mM sodium phosphate (pH 7.2), 0.5 M NaCl, 20% glycerol, and 0.5 M imidazole]. The purified protein was flash-frozen in liquid nitrogen and stored at −80 °C. For the activity assay, the protein was exchanged into 50 mM phosphate buffer (pH 8.0) with a PD-10 column (Pharmacia) and concentrated with a Centricon-10 concentrator (Amicon). Protein concentrations were determined by the Bradford assay (Bio-Rad). Typically, 1 L of culture yielded 80 mg of purified PICS TEs and all the other mutants except for PICS TE E187N/R191E (40 mg yield). PICS TE R191E could not be expressed at detectable levels. PICS TE and mutants were stable at 4 °C in a 10 mg/mL stock solution [50 mM phosphate buffer (pH 8.0)].

Construction of the DEBS Module 3−(PICS)TE Construct. Since PICS TE2 exhibited the best activity among the three PICS TE proteins, it was used for construction of the chimeric DEBS module 3−(PICS)TE construct. The PICS *te2* DNA was amplified by PCR from *pikAIV* bp 3145−4041 using the forward primer 5′-GTG AGT **AAG CTT** TCC GGG GCC GAC ACC GGC G-3′ and the reverse primer 5′-AGT GAG T**CT CGA G**CT TGC CCG CCC CCT CGA TGC C-3′ to introduce *Hin*dIII and *Xho*I restriction sites (boldface) at the N-terminal and C-terminal ends of the insert, respectively. The resulting PCR product was digested with *Hin*dIII and *Xho*I and cloned into pHL3-88, a pET-21c (Novagen)-based vector with an *Spe*I site introduced between the *Eco*RI and *Hin*dIII sites, to generate plasmid pHL4-25a. The *Nde*I−*Spe*I fragment of plasmid pRSG34 (*22*) containing DEBS module 3 was cloned into *Nde*I- and *Spe*I-digested pHL4-25a to give plasmid pHL4-28, encoding the DEBS M3−(PICS)TE construct.

Expression and Purification of DEBS M3−(PICS)TE and DEBS M3−(DEBS)TE Constructs. Plasmids pRSG34 and pHL4-28 were individually transformed into *E. coli* BL21-CodonPlus(DE3)-RP (Stratagene) harboring the *sfp* phosphopantetheinyl transferase gene from *Bacillus subtilis* (*23*). The *sfp* gene product was required for phosphopantetheinylation of the apo-ACP (*22*). A 1 L culture was grown at 37 °C in a 3 L flask using LB medium supplemented with the appropriate concentration of antibiotics. Protein expression was induced by addition of 1 mM IPTG at an OD_{600} of 0.8. After induction, incubation was continued for 12 h at 20 °C. The purification procedure was the same as that previously described for the DEBS module 2−(DEBS)TE construct (*24*).

Kinetic Analysis of PICS TE and Its Mutants. The rate of hydrolysis of diketide-SNAC substrates **1**−**5** was followed by spectrometric observation of the formation of 5-thio-2-nitrobenzoate by reaction of released HSNAC with 5,5′-dithio-2-nitrobenzoic acid (DTNB). To establish the time course of the PICS TE-catalyzed hydrolysis, the assay mixture consisted of 50 mM phosphate buffer (pH 8.0), 10 μM PICS TE2, 2 mM substrate **1**, and 6% (v/v) DMSO in a total volume of 500 μL. The reaction mixture was incubated at 30 °C. At intervals of 3, 5, 10, 15, and 20 min, 90 μL samples were withdrawn and the reaction was quenched by mixing with 20 μL of 1 M HCl. The protein was removed using a 5000 MW cutoff filter (Amicon). The amount of free thiol formation was quantitated at 412 nm by mixing 50 μL of the ultrafiltrate with 20 μL of a saturated solution of DTNB in 50 mM phosphate buffer (pH 8.0) and 930 μL of 50 mM phosphate buffer (pH 8.0).

Steady state kinetic measurements were carried out in duplicate. Diketide substrates **1**−**4** were >98% pure as determined by ^{1}H NMR, while 3-ketodiketide **5** contained ca. 5% free *N*-acetylcysteamine. DMSO was used to solubilize each diketide-SNAC substrate. Stock solutions of each of the NAC thioesters were 250 mM in DMSO. Since the apparent activity of the PICS TE was sensitive to the concentration of added DMSO, the total DMSO concentration was adjusted to 6% (v/v) for each incubation. In a typical assay, 10 μM PICS TE was mixed with a series of concentrations of diketide-SNAC, ranging from 2 to 14 mM in 50 mM phosphate buffer (pH 8.0), in a total volume of 220 μL. In all cases, the total content of DMSO in the assay reaction mixture was adjusted to 6% (v/v) to eliminate variations due to DMSO. The assay mixture was incubated at 30 °C for 10 min. Two 90 μL aliquots were withdrawn at the same time, and each was mixed with 20 μL of 1 M HCl and the amount of liberated thiol quantitated by reaction with DTNB as described above. The measured reaction rates were corrected for DMSO inhibition as well as the rate of background chemical hydrolysis in the absence of TE. The data were fit to the Michaelis−Menten equation by nonlinear least-squares regression using Kaleidagraph software to calculate k_{cat} and K_m. In selected cases, such as for diketides **1** and **2** with PICS TE mutant E187N/R191E and ketodiketide **5** with DEBS TE, in which the K_m was beyond the limits of solubility of the diketide-SNAC substrate, the k_{cat}/K_m was calculated from the slope of v versus [S] at low substrate concentrations.

For determination of the pH dependence of the hydrolysis of diketide **1** by PICS TE and DEBS TE, assays were carried out as described above either in 50 mM HEPES at pH 7.0 or 7.6 or in 50 mM Tris at pH 8.0, 8.4, or 9.0, along with 6% (v/v) DMSO (total volume of 500 μL).

Determination of Kinetic Parameters for DEBS M3−(PICS)TE and DEBS M3−(DEBS)TE Constructs. Kinetic assays were carried out by a variation of the previously

published method (*20*, *24*). The incubation mixture contained 5 μM DEBS M3−(PICS)TE or DEBS M3−(DEBS)TE construct, 1−10 mM substrate **1**, with the total DMSO volume adjusted to 10% (v/v), 178 μM DL-[2-*methyl*-^{14}C]-methylmalonyl-CoA (0.94 mCi/mmol), 100 mM sodium phosphate buffer (pH 7.2), 20% glycerol, 2.5 mM DTT, and 2 mM EDTA in a total volume of 100 μL. The assay solution was incubated at 30 °C for 1 h, followed by extraction with ethyl acetate. The residue after evaporation of the solvent was dissolved in ethyl acetate and then applied to a silica TLC plate. The radioactive products were separated by TLC by developing with a 4:1 EtOAc/hexane mixture and analyzed by phosphoimaging (Bio-Rad), using appropriate calibration standards.

RESULTS

Expression and Purification of PICS TE Domains. The PICS TE is covalently linked to the C-terminal end of ACP6 by a short linker peptide of ca. 80 amino acids. Sequence alignments with homologous ACP-TE regions of other modular PKSs indicate only that this linker is variable in amino acid sequence and do not reveal the intrinsic N-terminus of the PICS TE domain. To establish the optimal domain boundary, we used PCR to amplify the PICS TE domain, employing three different primers to generate TE proteins that differed only in the length of their N-terminal peptides. In each case, the reverse primer included the natural C-terminal stop codon of PICS module 6. Each of the PCR amplicons was inserted into the expression vector pET-28a, and the resultant plasmids were used to transform *E. coli* BL21(DE3)/pLysS. Recombinant PICS TE1 included nearly the entire interdomain linker peptide, starting five amino acids downstream of ACP6. The start of PICS TE2 was chosen to be 29 amino acids downstream of ACP6, and that of PICS TE3 began 80 amino acids after ACP6. All three recombinant TE proteins carried an N-terminal His_6 tag.

Each of the recombinant PICS TE proteins was purified by nickel affinity chromatography to >95% homogeneity (cf. Figure S1, Supporting Information). Although this His_6 tag could be removed by treatment with thrombin, the hydrolytic activity of the resultant thioesterases was the same either with or without the His_6 tag (data not shown). For convenience, therefore, all subsequent kinetic analyses were carried out without removal of the N-terminal His_6 tag. Among the three PICS TE constructs, PICS TE2 had the highest activity for hydrolysis of diketide **2**. By comparison, PICS TE1 had one-fifth the activity of PICS TE2, and PICS TE3 was inactive. All further experiments were therefore carried out on PICS TE2, henceforth simply termed PICS TE.

Steady State Kinetic Analysis of PICS TE. The thioesterase activity of PICS TE was assayed using a variation of the protocol originally described by Gokhale et al. for assay of the DEBS TE domain (*14*). In this latter procedure, release of the *N*-acetylcysteamine was continuously assessed by titration of the released free thiol with Ellman's reagent (5,5′-dithio-2-nitrobenzoic acid) and spectrophotometrically monitoring the formation of the resultant 5-thio-2-nitrobenzoic acid (λ_{max} = 412 nm, ϵ = 13 600 M^{-1} cm^{-1}). We found, however, that this continuous assay could not be used for PICS TE since the protein was rapidly inactivated in the presence of DTNB. Indeed, PICS TE could be titrated with 2 equiv of DTNB to give inactive enzyme, most likely by reaction with Cys48, which is found at the protein surface, and with Cys74, which is found in the interior of the protein (*18*). Although Cys73 of DEBS TE occupies a position analogous to that of Cys74 of PICS TE, exposure to DTNB does not appear to have a deleterious effect on DEBS TE, perhaps due to formation of an internal disulfide with the neighboring Cys72 (*17*). We therefore used a discontinuous assay for PICS TE activity, by quenching each reaction with 1 M HCl, removing proteins by ultrafiltration, and adding excess DTNB to the filtrate. Quenching at five different time points between 3 and 20 min established that the reaction was linear over this reaction period (data not shown), allowing the use of a single time point (10 min) for all subsequent kinetic assays.

Table 1: Steady State Kinetic Parameters for PICS TE and DEBS TE with Diketides **1**−**5**[a]

substrate		k_{cat} (min^{-1})	K_M (mM)	k_{cat}/K_M (M^{-1} s^{-1})
1	PICS TE	7.9 ± 0.6	21 ± 2	6.3 ± 0.8
	DEBS TE[b]	0.68 ± 0.16	9.6 ± 4.5	1.2 ± 0.6
2	PICS TE	4.3 ± 0.1	7.3 ± 0.5	9.8 ± 0.7
	DEBS TE[b]	6.6 ± 0.8	21 ± 4	5.3 ± 1.2
3	PICS TE	1.8 ± 0.2	16 ± 2	1.9 ± 0.3
4	PICS TE	2.6 ± 0.3	13 ± 2	3.3 ± 0.6
5	PICS TE	56 ± 7	15 ± 3	62 ± 15
	DEBS TE[c]	nd	nd	8.8 ± 0.9

[a] Data obtained by the one-point assay method. [b] DEBS TE (*16*): **1**, k_{cat}/K_m = 0.04 M^{-1} s^{-1}; **2**, k_{cat} = 12.2 min^{-1}, k_{cat}/K_m = 0.60 M^{-1} s^{-1}. [c] Measured as the initial slope of the plot of v vs [S]; nd, not determined.

Table 2: pH Dependence of the Hydrolysis of Thioester **1** by PICS TE and DEBS TE

	pH 7.0	pH 7.6	pH 8.0	pH 8.4	pH 9.0
PICS TE initial rate (A_{412}/min)	0.0011	0.0036	0.0047	0.0048	0.0021
DEBS TE k_{cat}/K_M (M^{-1} s^{-1})	−	−	5.2	−	3.8

The hydrolytic activity of PICS TE was determined for substrates **1**−**4**, the four diastereomers of the diketide analogue 2-methyl-3-hydroxypentanoyl-SNAC, as well as for racemic 2-methyl-3-ketopentanoyl-SNAC (**5**). For comparison, the specificity of DEBS TE for **1**, **2**, and ketoester **5** was also determined using the same one-point assay. In a control experiment, it was found that continuous monitoring of the rate of hydrolysis of 2 mM **2** by DEBS TE gave results that were the same as those obtained with the discontinuous, single-point assay. The observed steady state parameters are summarized in Table 1. PICS TE hydrolyzed the *syn*-diketide substrates **1** and **2** 2−5 times more rapidly than did DEBS TE. The preparation of DEBS TE used in these experiments had an apparent 20-fold higher specific activity than the enzyme preparation used in our previously reported studies of DEBS TE specificity (*14*), perhaps due to differences in the precise buffer composition or simply in the details of protein preparation.[2] Although the k_{cat} for hydrolysis of the (2*S*,3*R*)-diketide **1** by PICS TE was roughly double that for (2*R*,3*S*)-diketide **2**, the K_m for **2** was $^1/_3$ of that for **1**, resulting in a 1.6-fold greater specificity constant, k_{cat}/K_m, for **2** than for **1**. This narrow preference for **2** can be compared with the more pronounced 4.4-fold preference for **2** over **1** exhibited by DEBS TE. [Our earlier experiments with

Table 3: Steady State Kinetic Parameters for Diketides **1**, **2**, and **5** with Wild-Type and Mutant PICS TE

substrate		k_{cat} (min^{-1})	K_M (mM)	k_{cat}/K_M (M^{-1} s^{-1})	$[(k_{cat}/K_M)_{mutant}]/[(k_{cat}/K_M)_{WT}]$
1	WT[a]	7.9 ± 0.6	21 ± 2	6.3 ± 0.8	1
	S148A	inactive	inactive	inactive	inactive
	D176N	0.097 ± 0.009	4.6 ± 1.1	0.35 ± 0.03	0.056
	E187N	7.3 ± 0.6	14.7 ± 2.9	8.3 ± 1.8	1.32
	E187N/R191E[b]	nd	nd	0.94 ± 0.9	0.15
	R191N	2.6 ± 0.2	6.7 ± 1.1	6.5 ± 1.1	1.03
2	WT[a]	4.3 ± 0.1	7.3 ± 0.5	9.8 ± 0.7	1
	S148A	inactive	inactive	inactive	inactive
	D176N	0.17 ± 0.01	0.86 ± 0.22	3.3 ± 0.9	0.34
	E187N	7.8 ± 0.3	10.8 ± 0.8	12.0 ± 1.0	1.22
	E187N/R191E[b]	nd	nd	0.52 ± 0.05	0.05
	R191N	1.73 ± 0.06	2.6 ± 0.3	11.1 ± 1.3	1.13
5	WT[a]	56 ± 7	15 ± 3	62 ± 15	1
	D176N	2.1 ± 0.2	3.3 ± 0.8	10.6 ± 2.8	0.17
	E187N	85 ± 14	30.2 ± 6.7	47 ± 13	0.76
	E187N/R191E	2.6 ± 0.2	5.5 ± 0.1	7.9 ± 0.6	0.13
	R191N	17.3 ± 1.2	7.0 ± 1.1	41 ± 7	0.66

[a] Data taken from Table 1. [b] Measured as the initial slope of a plot of v vs [S]; nd, not determined.

nominally less active preparations of DEBS TE had shown an apparent 15-fold preference for **2** over **1** (*14*).] PICS TE hydrolyzed the two *anti*-diketide-SNAC substrates **3** and **4** with only modest 3- and 5-fold reductions in k_{cat}/K_m, respectively, compared to that of **2**. Notably, the ketoester **5** was the preferred substrate for PICS TE, exhibiting a k_{cat}/K_m more than 6-fold greater than that of the most active reduced diketide substrate **2**. By comparison, DEBS TE displayed only a 1.5-fold preference for hydrolysis of ketoester **5** over hydroxyester **2**. We also examined the pH dependence of the hydrolysis of **1** by both PICS TE and DEBS TE from pH 7.0 to 9.0. As summarized in Table 2, PICS TE displayed a pH optimum between pH 8.0 and 8.4, while DEBS TE also showed a preference for pH 8.0.

Activity of PICS TE Mutants. On the basis of sequence alignments as well as the structure of PICS TE (*18*), S148, H268, and D176 appear to comprise a catalytic triad that has the same geometry and hydrogen-bond interactions as other α/β-hydrolases (*25*−*28*). To test the proposed function of this presumed catalytic triad, PICS TE mutants S148A and D176N were generated and purified to homogeneity. PICS TE S148A did not hydrolyze either diketide **1** or **2** within the sensitivity limits of the DTNB assay which was capable of detecting a reduction in activity of at least 10^3 (Table 3). In contrast, the D176N mutant retained significant albeit reduced thioesterase activity. For example, while the k_{cat} for **2** was reduced 20-fold compared to that of wild-type PICS TE, this reduction in the maximal rate of hydrolysis was offset by an 8.5-fold reduction in K_m, resulting in a net only 3-fold reduction in k_{cat}/K_m. The reduction in catalytic efficiency toward **1** was somewhat more pronounced, with a 50-fold reduction in k_{cat} and a net 18-fold reduction in k_{cat}/K_m. The k_{cat} for the preferred diketide ketoester **5** was similarly reduced by a factor of 27, with only a 6-fold reduction in k_{cat}/K_m due to a compensating ca. 5-fold decrease in K_m.

PICS TE ^{184}EPI**E**VWS**R**QL

DEBS TE ^{177}DAM**N**AWL**E**EL

FIGURE 4: Partial sequence alignment between α-helix 6 of PICS TE and that of DEBS TE. Asn180 and Glu184 in DEBS TE are the counterparts of Glu187 and Arg191, respectively, in PICS TE.

Computational docking of 6-deoxyerythronolide B (6-dEB) with the active site of DEBS TE had previously led to the inference that amino acid residues N180 and E184 interact with the C-3 and C-5 hydroxyl groups, respectively, of 6-dEB (*17*). Both primary amino acid sequence and three-dimensional structural alignments suggest that these two residues correspond to E187 and R191 of PICS TE, which appear to be capable of forming hydrogen bonds with the C-3 carbonyl and C-5 hydroxyl of narbonolide (*18*) (Figure 4). To examine the possible influence of these two amino acids on substrate specificity, we used site-directed mutagenesis to generate a series of PICS TE mutants, E187N, E187N/R191E, and R191N, and investigated the hydrolysis of diketides **1**, **2**, and **5** by these mutants (Table 3). Attempts to obtain PICS TE mutant R191E were unsuccessful.

Substitution of asparagine for glutamate in the E187N mutant of PICS TE resulted in only relatively minor changes in both the absolute and relative values of the steady state kinetic parameters for diketides **1**, **2**, and **5**. The 3-ketoacyl thioester **5** was still preferred over 3-hydroxyacyl thioesters **1** and **2**, by factors of ∼6 and ∼4, respectively, based on k_{cat}/K_m values, only slightly less than the observed 10- and 6-fold preferences, respectively, determined for the wild-

[2] A referee has asked for clarification of the differences between the methods for expression, purification, and assay of DEBS TE reported in ref *14* and those used in the current study. Gokhale et al. induced protein production at an OD_{595} of 0.6 and allowed the cultures to continuously grow for an additional 14 h before harvesting. We induced protein production at an OD_{600} of 0.8 and grew the cultures for a further 12 h at 20 °C. Gokhale et al. disrupted cells in 100 mM Tris (pH 8.4) with no other additives. We disrupted cells in 200 mM sodium phosphate (pH 7.2) which contained DTT, and the protease inhibitors benzamidine, pepstatin, and leupeptin, as well as 30% glycerol. Gokhale et al. did not precipitate DNA. We first digested DNA with DNaseI followed by polyethylenimine precipitation. Gokhale et al. used a Qiagen Ni−agarose column to purify protein followed by buffer exchange using a Centripep 10 apparatus (Amicon). We used His-Bind resin from Novagen and a PD10 (Pharmacia) column for buffer exchange. Both Gokhale et al. and we carried out kinetic assays in 50 mM phosphate (pH 8.0). Although we have not investigated the precise reasons for the improved activity of the recombinant DEBS TE, the activity difference most likely lies in the buffer used for cell disruption which contained both protease inhibitors and the antioxidant DTT, thereby preventing the possible loss of enzyme activity during and immediately after cell disruption.

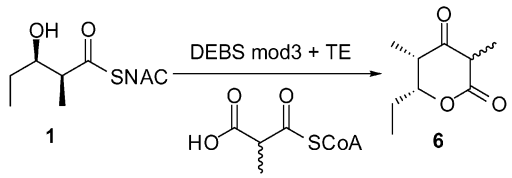

FIGURE 5: Formation of triketide ketolactone **6** from diketide **2** catalyzed by DEBS module 3 being fused to DEBS TE or PICS TE.

Table 4: Steady State Kinetic Parameters for Formation of Triketide Lactone **6** by DEBS Module 3 Fused to DEBS TE or PICS TE

	k_{cat} (min^{-1})	K_M (mM)	k_{cat}/K_M (M^{-1} s^{-1})
DEBS M3−(DEBS)TE	0.054 ± 0.003	4.3 ± 0.5	0.22 ± 0.3
DEBS M3−(PICS)TE	1.16 ± 0.04	1.84 ± 0.05	10.5 ± 0.4

type PICS TE. Although we were unable to express the PICTS TE R191E mutant, the corresponding E187N/R191E double mutant displayed a 10-fold reduction in the k_{cat}/K_m for ketoester **5**, while retaining a clear relative preference for **5** over both **1** (~8-fold) and **2** (~15-fold). Interestingly, the 2:1 preference of E187N/R191E PICS TE for **1** over **2** was the reverse of that shown by the wild-type thioesterase. Finally, the absolute and relative steady state kinetic parameters for the R197N mutant were comparable to those determined for the E197N variant.

Fusion of DEBS Module 3 to PICS TE. When DEBS TE is fused to the C-terminus of DEBS module 3, the resultant DEBS M3−(DEBS)TE fusion will convert diketide **1** and methylmalonyl-CoA to the triketide ketolactone **6** (*22*) (Figure 5). The substrate for the lactonization catalyzed by the appended DEBS TE domain is the 2,4-methyl-3-keto-5-hydroxy triketide acyl-ACP thioester. Since **5**, the preferred model substrate for PICS TE, is itself a 2-methyl-3-keto diketide acyl thioester, we reasoned that PICS TE might have advantages over DEBS TE for release of ketoester substrates from intact PKS modules. To test this idea, we therefore used domain swapping to generate the DEBS M3−(PICS)TE construct, in which the heterologous PICS TE has replaced the homologous DEBS TE. The resultant chimeric enzyme catalyzed the formation of **6** with a k_{cat} more than 20-fold greater than that of the DEBS M3−(DEBS)TE construct and a k_{cat}/K_m nearly 50 times greater (Table 4).

DISCUSSION

To determine the optimal N-terminal domain boundary, we first expressed the PICS TE domain with three different N-terminal peptides, representing different starting points within the ~80-amino acid peptide linker between the PICS ACP6 and TE domains. Of the three constructs, the intermediate length PICS TE2, with a start codon 29 amino acids downstream of the end of the ACP domain, was the most active, with PICS TE1, which carried an additional 24 amino acids at the N-terminus, found to be one-fifth as active and PICS TE3, which was truncated by an additional 51 amino acids compared to PICS TE2, found to be completely inactive. The crystal structure of PICS TE2 shows that the protein is a dimer, with the hydrophobic dimer interface resulting from the interaction of a pair of N-terminal α-helices (*18*). Interestingly, protein secondary structure predictions made using the program NNPREDICT[3] suggest that the additional 24 amino acids in PICS TE1 compared to PICS TE2 could form a nine-amino acid α-helix that might interfere with dimer formation, while deletion of another 51 amino acids in PICS TE3 would abolish this interface altogether.

Native PICS TE is located at the C-terminus of PICS module 6 and is unusual as a PKS thioesterase in that it normally lactonizes both a (2*R*)-2-methyl-3-ketoacyl heptaketide thioester, covalently attached to ACP6, and a (2*R*,3*S*)-2-methyl-3-hydroxyacyl hexaketide thioester that is generated attached to PICS ACP5 (*3*, *4*, *7*). Truncation of the N-terminal portion of PICS KS6 results in the exclusive formation of the hexaketide lactone, although there are no data yet available that show whether full-length PICS module 6 naturally lactonizes both substrates or only the full-length heptaketide (*7*). Under natural circumstances, PICS TE does not encounter any of the other three diastereomers of its 2-methyl-3-hydroxyacyl thioester substrate. Comparison of diketide-SNAC thioester analogues **1**−**4** reveals a small but real diastereomeric preference for the (2*R*,3*S*)-**2** diastereomer, with the k_{cat}/K_m preference in the following order: **2** > **1** > **4** > **3**. The configuration of the 3-hydroxyl is thus apparently slightly more important to k_{cat}/K_m than the configuration of the 2-methyl group. The preference for **2** over **1** is less pronounced than that shown by DEBS TE for the same pair of diketide diastereomers. The (racemic) 3-keto-2-methyl-acyl-SNAC **5** is the preferred substrate for PICS TE, with a 6-fold preference over the best reduced diketide **2**. Interestingly, DEBS TE also shows a slight preference for the ketoester **5** over **2**, but by a more modest factor of 1.5. Mutation of the E187 and R191 residues of the PICS TE to match those of the DEBS TE had only relatively minor effects on the observed substrate specificity toward **1**, **2**, and **5**. The overall difference in substrate specificity between DEBS TE (k_{cat}/K_m, **5** = **2** > **1**) and PICS TE (k_{cat}/K_m, **5** ≫ **2** > **1**) may reflect the combination of the effects of the intrinsic reactivity of the substrate (**5** > **1** and **2**) and the specific molecular recognition by each TE of the substitution pattern and stereochemistry of its cognate substrate. Comparisons of the PICS TE and DEBS TE protein structures are reported in the following paper (*18*).

PICS TE, along with DEBS TE and other members of the α/β-hydrolase superfamily, has an apparent characteristic catalytic triad consisting of serine 148, histidine 268, and aspartate 176 (*25*−*28*). Consistent with this idea is the finding that the PICS TE S148A mutant was catalytically inactive toward both **1** and **2**. In contrast, the D176N mutant retained substantial, although reduced, hydrolytic activity toward **1**, **2**, and **5**. This may indicate that D176 is not part of a true catalytic triad or, more likely, that it acts in a manner different from that of the aspartate residue in the canonical catalytic triad of the serine proteases and α/β-hydrolases where the replacement of aspartate with asparagine can result in a decrease in k_{cat} by a factor of 10 000. Interestingly, for trypsin, the magnitude of the effect of the D105N substitution is modulated by increasing the pH, with the 10000-fold decrease in k_{cat} at pH 7.0 being reduced to only 15-fold at pH 10 (*29*). Notably, in the outer membrane phospholipase A of *E. coli*, the catalytic triad naturally contains asparagine

[3] http://www.cmpharm.ucsf.edu/~nomi/nnpredict.html.

(*30*), although this protein does not have the α/β-hydrolase fold. In a more distantly related enzyme system, replacement of Asp121 with Asn in the catalytic diad of bovine pancreatic ribonuclease A resulted in only a modest decrease in phosphodiesterase activity (*31*).

The enhanced specific activity and broad substrate specificity of PICS TE compared to those of DEBS TE make PICS TE an attractive component of the tool kit for engineering chimeric PKS modules with superior catalytic properties. Indeed, the hybrid module with PICS TE fused to the C-terminus of heterologous DEBS module 3 catalyzed the formation of triketide ketolactone **6** at a rate considerably higher than that observed for the previously described DEBS module 3−(DEBS)TE construct. This apparent increase in catalytic efficiency, as measured by the value of k_{cat}/K_m, cannot be ascribed simply to the greater preference of PICS TE for ketoacyl thioester substrates, however, since k_{cat}/K_m, which only reflects kinetic events up to and including the first irreversible step, cannot be influenced by reactions occurring after the irreversible KS-catalyzed chain elongation reaction. On the other hand, the k_{cat} of the DEBS M3−(PICS)TE construct is 20-fold larger than that of the DEBS M3−(DEBS)TE construct. This is consistent with the observation that the stand-alone PICS TE domain has a k_{cat} 11-fold greater than that of the stand-alone DEBS TE domain. This result implies that part of the rate acceleration observed in the chimeric DEBS M3−(PICS)TE construct versus the DEBS M3−(DEBS)TE construct may reflect the increased rate of release of the enzyme-bound triketide by TE-catalyzed lactonization. Whatever the origin, the improved kinetic behavior of the chimeric module carrying PICS TE has practical utility for engineering of hybrid PKS systems (*1*, *2*).

ACKNOWLEDGMENT

We thank Dr. Robert McDaniel of Kosan Biosciences for a gift of plasmid pKOS039-86 harboring the PICS PKS.

SUPPORTING INFORMATION AVAILABLE

Primers and amplification conditions for PCR mutagenesis of PICS TE and SDS−PAGE analysis of PICS TE purification. This material is available free of charge via the Internet at http://pubs.acs.org.

REFERENCES

1. Cane, D. E., Walsh, C. T., and Khosla, C. (1998) *Science 282*, 63−68.
2. Khosla, C., Gokhale, R. S., Jacobsen, J. R., and Cane, D. E. (1999) *Annu. Rev. Biochem. 68*, 219−253.
3. Xue, Y., Zhao, L., Liu, H. W., and Sherman, D. H. (1998) *Proc. Natl. Acad. Sci. U.S.A. 95*, 12111−12116.
4. Tang, L., Fu, H., Betlach, M. C., and McDaniel, R. (1999) *Chem. Biol. 6*, 553−558.
5. Staunton, J., and Wilkinson, B. (1997) *Chem. Rev. 97*, 2611−2629.
6. Lambalot, R. H., and Cane, D. E. (1992) *J. Antibiot. 45*, 1981−1982.
7. Xue, Y., and Sherman, D. H. (2000) *Nature 403*, 571−575.
8. Betlach, M. C., Kealey, J. T., Ashley, G. W., and McDaniel, R. (1998) *Biochemistry 37*, 14937−14942.
9. Graziani, E. I., Cane, D. E., Betlach, M. C., Kealey, J. T., and McDaniel, R. (1998) *Bioorg. Med. Chem. Lett. 8*, 3117−3120.
10. Xue, Y., Wilson, D., Zhao, L., Liu, H., and Sherman, D. H. (1998) *Chem. Biol. 5*, 661−667.
11. Borisova, S. A., Zhao, L., Sherman, D. H., and Liu, H. W. (1999) *Org. Lett. 1*, 133−136.
12. Kao, C. M., Luo, G., Katz, L., Cane, D. E., and Khosla, C. (1995) *J. Am. Chem. Soc. 117*, 9105−9106.
13. Jacobsen, J. R., Hutchinson, C. R., Cane, D. E., and Khosla, C. (1997) *Science 277*, 367−369.
14. Gokhale, R. S., Hunziker, D., Cane, D. E., and Khosla, C. (1999) *Chem. Biol. 6*, 117−125.
15. Aggarwal, R., Caffrey, P., Leadlay, P. F., Smith, C. J., and Staunton, J. (1995) *J. Chem. Soc., Chem. Commun.*, 1519−1520.
16. Weissman, K. J., Smith, C., Hanefield, U., Aggarwak, R., Bycroft, M., Staunton, J., and Leadlay, P. F. (1998) *Angew. Chem., Int. Ed. 37*, 1437−1440.
17. Tsai, S. C., Miercke, L. J., Krucinski, J., Gokhale, R., Chen, J. C., Foster, P. G., Cane, D. E., Khosla, C., and Stroud, R. M. (2001) *Proc. Natl. Acad. Sci. U.S.A. 98*, 14808−14813.
18. Tsai, S.-C., Lu, H., Cane, D. E., Khosla, C., and Stroud, R. M. (2002) *Biochemistry 41*, 12598−12606.
19. Cane, D. E., Lambalot, R. H., Prabhakaran, P. C., and Ott, W. R. (1993) *J. Am. Chem. Soc. 115*, 522−526.
20. Wu, N., Kudo, F., Cane, D. E., and Khosla, C. (2000) *J. Am. Chem. Soc. 122*, 4847−4852.
21. Gilbert, I. H., Ginty, M., O'Neill, J. A., Simpson, T. J., Staunton, J., and Willis, C. L. (1995) *Bioorg. Med. Chem. Lett. 5*, 1587−1590.
22. Gokhale, R. S., Tsuji, S. Y., Cane, D. E., and Khosla, C. (1999) *Science 284*, 482−485.
23. Lambalot, R. H., Gehring, A. M., Flugel, R. S., Zuber, P., LaCelle, M., Marahiel, M. A., Reid, R., Khosla, C., and Walsh, C. T. (1996) *Chem. Biol. 3*, 923−936.
24. Cane, D. E., Kudo, F., Kinoshita, K., and Khosla, C. (2002) *Chem. Biol. 9*, 131−142.
25. Lawson, D. M., Derewenda, U., Serre, L., Ferri, S., Szittner, R., Wei, Y., Meighen, E. A., and Derewenda, Z. S. (1994) *Biochemistry 33*, 9382−9388.
26. Bellizzi, J. J., III, Widom, J., Kemp, C., Lu, J. Y., Das, A. K., Hofmann, S. L., and Clardy, J. (2000) *Proc. Natl. Acad. Sci. U.S.A. 97*, 4573−4578.
27. Devedjiev, Y., Dauter, Z., Kuznetsov, S. R., Jones, T. L., and Derewenda, Z. S. (2000) *Struct. Folding Des. 8*, 1137−1146.
28. Bruner, S. D., Weber, T., Kohli, R. M., Schwarzer, D., Marahiel, M. A., Walsh, C. T., and Stubbs, M. T. (2002) *Structure 10*, 301−310.
29. Craik, C. S., Roczniak, S., Largman, C., and Rutter, W. J. (1987) *Science 237*, 909−913.
30. Kingma, R. L., Fragiathaki, M., Snijder, H. J., Dijkstra, B. W., Verheij, H. M., Dekker, N., and Egmond, M. R. (2000) *Biochemistry 39*, 10017−10022.
31. Quirk, D. J., and Raines, R. T. (1999) *Biophys. J. 76*, 1571−1579.

BI026006D